# Synergistic drug combination effectively blocks Ebola virus infection

**Wei Sun**[#1], **Shihua He**[#2,3], **Carles Martínez-Romero**[#4,5], **Jennifer Kouznetsova**[1], **Gregory Tawa**[1], **Miao Xu**[1], **Paul Shinn**[1], **Ethan Fisher**[1], **Yan Long**[1], **Omid Motabar**[1], **Shu Yang**[1], **Philip E. Sanderson**[1], **Peter R. Williamson**[6], **Adolfo García-Sastre**[4,5,7,*], **Xiangguo Qiu**[2,3,*], and **Wei Zheng**[1,*]

[1]National Center for Advancing Translational Sciences, National Institutes of Health, 9800 Medical Center Drive, Bethesda MD 20892, USA

[2]Special Pathogens Program, National Microbiology Laboratory, Public Health Agency of Canada, Winnipeg, Manitoba R3E 3R2, Canada

[3]Department of Medical Microbiology, University of Manitoba, Winnipeg, Manitoba R3E 0J9, Canada

[4]Department of Microbiology, Icahn School of Medicine at Mount Sinai, New York, NY 10029, USA

[5]Global Health and Emerging Pathogens Institute, Icahn School of Medicine at Mount Sinai, New York, NY 10029, USA

[6]Laboratory of Clinical Infectious Diseases, National Institute of Allergy and Infectious Diseases, National Institutes of Health, Bethesda, MD, 20892, USA

[7]Department of Medicine, Division of Infectious Diseases, Icahn School of Medicine at Mount Sinai, New York, NY 10029, USA

[#] These authors contributed equally to this work.

## Abstract

Although a group of FDA-approved drugs were previously identified with activity against Ebola virus, most of them are not clinically useful because their human blood concentrations are not high enough to inhibit EBOV infection. We screened 795 unique three-drug combinations in an EBOV entry assay. Two sets of three-drug combinations, toremifene-mefloquine-posaconazole and toremifene-clarithromycin-posaconazole, were identified that effectively blocked EBOV entry and

[*]To whom correspondence may be addressed. Adolfo García-Sastre, Ph.D., Department of Microbiology, Icahn School of Medicine at Mount Sinai, 1468 Madison Avenue, New York, NY 10029, Adolfo.Garcia-Sastre@mssm.edu, Tel.: (212) 241-7769, Xiangguo Qiu, M.D., Special Pathogens Program, National Microbiology Laboratory, Public Health Agency of Canada, 1015 Arlington Street, Winnipeg, MB R3E 3R2 Canada, xiangguo.qiu@phac-aspc.gc.ca, Tel.: (204) 784-7548, Wei Zheng, Ph.D., National Center for Advancing Translational Sciences, National Institutes of Health, 9800 Medical Center Drive, Bethesda, MD 20892-3375, wzheng@mail.nih.gov, Tel.: (301)217-5251.

Conflict of interests: none.

were further validated for inhibition of live EBOV infection. The individual drug concentrations in the combinations were reduced to clinically relevant levels. We identified mechanisms of action of these drugs: functional inhibitions of Niemann–Pick C1, acid sphingomyelinase, and lysosomal calcium release. Our findings identify the drug combinations with potential to treat EBOV infection.

## Keywords

Ebola treatment; Ebola prevention; Drug combination; Drug repurposing; polypharmacology

## 1. Introduction

The EBOV entry pathway has been extensively studied (Jae and Brummelkamp, 2015; Moller-Tank and Maury, 2015), although a few components involved at the early and the late stages are still unknown. Macropinocytosis and endocytosis have been implicated in EBOV entry and intracellular trafficking. Involvements of cathepsin B/L (Chandran et al., 2005), Niemann Pick C1 protein (NPC1) (Carette et al., 2011; Cote et al., 2011), acid sphingomyelinase (ASM) (Miller et al., 2012), and two-pore channel (TPC) (Sakurai et al., 2015) in EBOV entry have been reported. Cathepsin B/L proteolytically hydrolyzes EBOV glycoprotein (GP) to trigger subsequent downstream infection events and cathepsin inhibition blocks EBOV replication. The hydrolyzed EBOV GP binds to NPC1 activating lysosome escape and virus genome injection to cytoplasm where viral replication occurs. Fibroblasts derived from patients deficient in NPC1 and NPC1 knock-out mice showed resistance to EBOV infection (Herbert et al., 2015). More recently, tetrandrine, a small molecule inhibitor of TPCs, showed a moderate protection in the EBOV mouse model (Sakurai et al., 2015).

Our previous drug repurposing screen identified 53 FDA approved drugs that blocked Ebola virus-like particle (VLP) entry but the concentrations required for most of them were over the maximum blood concentrations of these drugs in human (Kouznetsova et al., 2014). In pharmacokinetic studies, the maximum drug concentration in human blood or plasma is the peak drug concentration detected after the drug is administrated in an *in vivo* experiment. Weak potency and insufficient plasma concentration are the common issues encountered for the active compounds found from drug repurposing screens (Sun et al., 2016). In this study, we report a targeted drug combination approach and identification of unique three-drug combinations that synergistically block EBOV infection. The reduced individual drug concentrations in the combinations are reachable in human plasma. Further, we validated their inhibitions of live virus infection in cells and identified their mechanisms of inhibition. These drug combinations may have a potential for the treatment of EBOV infection.

## 2. Materials and Methods

### 2.1.Materials

Ebola VLPs containing a beta-lactamase-fused VP40 protein (EBOV BlaVP40) and GP were produced in Dr. García-Sastre's lab, as previously described (Tscherne et al., 2010).

LiveBLAzer FRET–B/G Loading Kit with CCF2-AM were purchased from Life Technologies (Carlsbad, CA, USA); eGFP-EBOV was produced as previously described (Johansen et al., 2013). Constructs of RFP organelle marker were purchased from Thermo Fisher Scientific. An ATP content cell viability assay kit was purchased from Promega (Madison, WI, USA). Polystyrene plates (384-well and 1536-well black, clear bottom, sterile, tissue culture treated) were purchased from Greiner Bio-One (Monroe, NC, USA). The compounds were purchased from Sigma (St. Louis, MO, USA) at the highest available purity.

### 2.2. Ebola VLP beta-lactamase assays for combination HTS in 1536-well plate

The Ebola VLP assay was performed as described previously (Kouznetsova et al., 2014). Briefly, the first drug and the second drug were premixed assay medium and 0.8 μl of this mixture was then transferred into assay plate containing Hela cells; 23 nl of the third drug was transferred into the assay plate. The cells were treated with 1 μl/well VLP. The CCF2-AM beta-lactamase substrate was added and fluorescence intensities were measured using an Envision plate reader.

### 2.3. Ebola live virus assays

Vero E6 cells were plated in the 96-well plate (black with optical bottom). Briefly, serial dilutions of 7 drugs (diluted in DMEM 2% FBS starting at 46 μM) and combinations, and DMSO as control, were added to the wells, and incubated for 1 hr at 37°C with 5% $CO_2$. The cells were infected with EBOV/Mayinga-eGFP at a MOI of 0.1 TCID50/cell. The assay was run in triplicate. The fluorescence was read 72 hr after infection using a BioTek Synergy HT.

### 2.4. NAADP stimulated calcium release

Fibroblasts (GM05659) were seeded on 96-well plates (3000 cells/well). The cells were loaded with Nuc. Blue live staining dye (Invitrogen) and incubated for 15 mins. The cells were washed twice before loading with Cal-520-AM (AAT-Bioquest, CA) as previously described (Xu et al., 2012b). The cells were treated with each drug at 37°C for 2 hr. Once mounted on the microscope, the reaction of cells to NAADP-AM (10 μM) or vehicle DMSO was monitored by capturing images every 1 sec for a total of 180 secs. Cal-520 fluorescence was then measured per cell using INCell Analyzer 2200 and analyzed by INCell Analyzer workstation software.

### 2.5. Co-localization assay

U2OS cells were seeded on 96-well plates (3000/100ul/well). Medium was removed after 24 hrs. The cells were transfected with 0.5-1.5 μ L/well of RFP-plasma membrane, RFP-early endosomes, RFP-late endosomes, and RFP-lysosomes and incubated for 24 hr. The cells were washed with medium, treated with 50 μl drug for 1 hr at 37°C, infected with 50 μl eGFP-EBOV, and then incubated at 37°C for 4 hr. The medium was removed and the cells were stained with nuclear dye for 30 mins. The fluorescence was then measured using IN Cell Analyzer 2200.

### 2.6.Cathepsin B/L assay

Cathepsin L (Novus Biologicals, Littleton, CO) was reconstituted with reaction buffer. 5 ng of cathpsin L was added into each well in 384-well plate. Indicated drugs were added into cathpsin L and premixed for 29 min. 200 uM cathepsin L substrate Ac-FR-AFC (Abcam) was added to initiate the reaction. Fluorescence was measured using Tecan Infinite M1000 Pro (Ex=400±20, Em=505±20). Cathepsin L inhibitor was used as a positive control. The cathepsin B (Abcam) was assayed in the same manner as cathepsin L, but with the cathepsin B substrate Ac-RR-AFC (Abcam) in the presence of cathepsin B inhibitor Z-FA-FMK.

### 2.7. Functional assays for NPC1 (Amplex-red), acid sphingomyelinase (ASM), Filipin staining and Lysotracker-red staining.

Amplex-red cholesterol assay, Filipin assay and Lysotracker-red assay was performed as previously described (Xu et al., 2012b). ASM assay was performed previously described (Xu et al., 2012a).

### 2.8. Data analysis and statistics

The primary screen data and curve fitting were analyzed using software developed internally at the NIH Chemical Genomics Center (NCGC) (Wang et al., 2010). Heat map of triple drug combinations where rows enumerate drug 1, columns enumerate drugs 2, 3 and heat map elements are ratios defined as $AC_{50}$ (drug 1 alone)/ $AC_{50}$ (drugs $1 + 2 + 3$). The $AC_{50}$ values were computed by first normalizing the channel 0 signal to positive control and then correcting for background effects. Half maximal inhibitory concentration ($IC_{50}$) values and 95% CI of compound confirmation data were calculated using Prism software (GraphPad Software, Inc. San Diego, CA). Results in the figures are expressed as mean of triplicates ± SEM. Differences in Anti-EBOV activity between 3-drug treatment and single drug treatments were evaluated using student's t-test (two-tailed) to compare two groups and to calculate P values. In the figures, a p-value < 0.001 indicates a significant difference between experimental groups.

## 3. Results

### 3.1. Screening of synergistic drug combinations to reduce individual drug concentrations needed to inhibit EBOV infection

To overcome the weak activities of previously identified FDA-approved drugs against EBOV, we applied a targeted drug combination approach that selects individual drugs based on different mechanisms of action or therapeutic indications. We hypothesize that a combination therapy of three-drugs with different mechanisms of action will be able to block EBOV infection with lower individual drug concentrations due to the synergistic effect.

To increase the screening throughput for large numbers of three-drug combinations, we fixed two drugs at concentrations below their human $C_{max}$ (maximal concentration reached in plasma) and varied concentrations of the third drug by 1:3 dilutions. The synergistic effect in a drug combination was identified when the $IC_{50}$ value of the third drug decreases significantly (5-fold or more) compared to that in its single drug application. The 53

approved drugs previously identified (Kouznetsova et al., 2014) plus two other reported EBOV active drugs chloroquine (Madrid et al., 2013) and nilotinib (Garcia et al., 2012) were divided into three groups for designing different sets of three-drug combinations (SI Table 1). The first group of two drugs, toremifene and chloroquine, exhibited activity in the EBOV live virus assay and animal model (Johansen et al., 2013; Madrid et al., 2013). Group 2 consists of eight compounds that showed good efficacy in the VLP entry assay with preferred pharmacokinetic (PK) and toxicity profiles (SI Table 2). Group 3 contains all these 55 approved drugs (SI Table3). In the three-drug combinations, drug-1 and drug-2 were selected from groups 1 and 2 with drug concentration corresponding to their $C_{max}$ or $IC_{20}$ concentrations. The third drug from group 3 was tested at 11 concentrations from 0.001 to 57 μ M in combination with the other two drugs. A total of 795 unique three-drug combinations were tested in Ebola VLP beta lactamase assay (Figure 1A and SI Table 3). The VLP is comprised of glycoprotein (GP) and the matrix protein VP40 fused to a beta-lactamase reporter enzyme. This assay monitors VLP entry into cells when the reporter-enzyme hydrolyzes the FRET based substrate inside cells. This cell-based assay has been previously miniaturized into 1536 well format.

### 3.2. Identification of effective drug combinations from high throughput screening

Among drug combinations tested, 16 of them showed increased potency with the $IC_{50}$ values 5-fold or more potent in the three-drug combinations than these in the single drug application (Figure 1 A and SI Table 3). Three sets of three-drug combination blocked greater than 90% Ebola VLPentry (Figure 1 and Table 1) and the individual drug concentrations were all below their $C_{max}$ values (Table 1). In the first two three-drug sets, 0.15 μ M toremifene plus 2 μM clarithromycin and 0.15 μM toremifene plus 2 μM mefloquine sensitized the third drug posaconazole for approximately 25 fold and 23 fold, respectively (Figure 1B and 1C). In the third set, 2 μM chloroquine with 1 μM maprotiline improved azithromycin for approximately 5 fold (Figure 1D). The activities of these combinations were further confirmed with a single third drug concentration (below their $C_{max}$ concentrations) (Figure 1E-G).

The inhibitory effects of three 3-drug combinations (toremifene-clarithromycin-posaconazole (TCP), toremifene-mefloquine-posaconazole (TMP), and chloroquine-maprotiline-azithromycin (CMA)) and of individual drugs in these combinations were then confirmed in a high content assay for inhibition of Ebola VLP entry (Figure 1H-K and SI Figure 1). In addition, three 2-drug combinations (toremifene–posaconazole, toremifene-mefloquine, and toremifene-clarithromycin) were also evaluated (SI Figure 2). Because the efficacy obtained in two-drug combinations was lower than that in three-drug combinations, they were not further tested.

Additionally, the cytotoxicity of these drugs and 3 drug combinations were evaluated in an ATP-content cell viability assay. Mefloquine showed partial cytotoxicity at 57 μ M, the other six compounds and 3 drug combinations were not cytotoxic (Figure 1L and SI Figure 3).

### 3.3. Validation of three-drug combinations in EBOV infection assay

The live EBOV infection assay is a useful *in vitro* model for validation of Ebola VLP entry inhibitors. Live EBOV infections require bio-safety level 4 (BSL4) containment. Vero E6 cells were treated with either individual drugs or three-drug combinations (TCP, TMP, or CMA) for one hr, followed by EBOV incubation for 72 hrs (Figure 2). Toremifene, posaconazole, mefloquine, and maprotiline individually showed dose-response inhibitions against EBOV infections (Figure 2B and Table 2). Clarithromycin inhibited 50% of EBOV infection at the highest tested concentration (46 μ M). Chloroquine and azithromycin were not active at highest tested concentrations (46 μM) in the live virus assays.

We then tested the three sets of three-drug combinations in the live EBOV infection assay. TCP showed markedly synergistic effect, inhibiting more than 90% EBOV infection, while the individual drugs at that such low concentrations were not active (Figure 2B). TMP blocked 74% EBOV infection (Figure 2C). However, CMA failed to block EBOV infection (Figure 2D). The results validated the anti-virus effect of TCP and TMP that were initially identified in the Ebola VLP assay. The results indicate that the TCP and TMP three-drug combinations are able to block EBOV infection *in vitro* at the clinically relevant drug concentrations.

Toremifene, clarithromycin, posaconazole, and mefloquine are the four drugs used in the TCP and TMP combinations. The mechanisms of action of these four compounds for inhibiting EBOV infection are unknown. We then performed mechanistic studies to explore their potential mechanisms of action.

### 3.4. Inhibition of NAADP stimulated lysosomal calcium release by toremifene, posaconazole, mefloquine, and clarithromycin

NAADP stimulated TPC involve calcium signaling in endosome and lysosome which has been implicated in the EBOV infection (Sakurai et al., 2015). Specifically, verapamil and tetrandrine were shown to block the calcium signaling triggered by NAADP, leading to inhibition of EBOV infection. To study the mechanisms of action of these four anti-EBOV drugs, the activities of these compounds on the lysosomal calcium release were measured in fibroblasts. Toremifene, clarithromycin, posaconazole, and mefloquine exhibited strong inhibition of NAADP-AM stimulated lysosomal calcium release (Figure 3A and SI Figure 4). The results indicate that the inhibitory effect of these compounds on NAADP stimulated lysosomal calcium release may contribute to their activity against EBOV infection.

### 3.5. Inhibition of EBOV entry at late endosome and lysosome stages by posaconazole

EBOV enters the cell through macropinocytotic uptake into the endosomal compartment (Jae and Brummelkamp, 2015) followed by traveling through the endocytosis pathway and exiting from late endosome/lysosome to the cytosol. We evaluated the co-localizations of EBOV with several key organelles involved in this pathway, including plasma membrane, early endosome, late endosome and lysosome. RFP-labeled protein marker and eGFP-EBOV were co-transfected into U2OS cells that were treated with these four compounds. None of the four drugs blocked the entry of EBOV at the stages of the plasma membrane and early endosome (Figure 3B). Interestingly, posaconazole showed phenotypes similar to cathepsin

B/L inhibitor (E-64 D) in the late endosomes and to NPC inhibitor (U18666A) in lysosomes, while the other three drugs did not have a similar effect (Figure 3B).

We then tested whether these four drugs could inhibit cathepsin B or L. After the recombinant cathepsin B or cathepsin L was treated with the compounds, a fluorescent substrate was added to initiate the protease reaction. We found that none of these four compounds could inhibit the activity of either cathepsin B or cathepsin L (Figure 3C and 3D). The negative result of toremifene was previously reported (Johansen et al., 2013).

### 3.6. Function of NPC1 impaired by posaconazole

We measured both free cholesterol and cholesteryl esters in HeLa cells in the presence of all the four compounds. Posaconazole dramatically increased cholesterol accumulation in lysosomes as measured by filipin staining (Figure 3F) with an $IC_{50}$ of 0.27 μM (95% CI: 0.21 to 0.35 μ M) in the Amplex-red cholesterol assay (Figure 3E). Posaconazole also increased the size of lysosomes visualized in the Lysotracker staining experiment (Figure 3G). The other three compounds did not induce cholesterol accumulations. Together, the results indicated that posaconazole impairs NPC1 protein function resulting in lysosomal cholesterol accumulation and enlargement of lysosome similar to the NPC disease phenotype.

### 3.7. Inhibition of ASM by posaconazole, toremifene, and mefloquine

The effect of these four compounds on the activity of ASM was then tested. We found that posaconazole inhibited ASM activity with a potent $IC_{50}$ value of 0.087 μM (95% CI: 0.034 to 0.21 μM) (Figure 3H). Toremifene also inhibited ASM activity with an $IC_{50}$ of 2.08 μM (95% CI: 1.20 to 6.64 μM) and mefloquine with an $IC_{50}$ of 1.65 μM (95% CI: 0.68 to 3.98 μ M) (Figure 3H). However, clarithromycin did not inhibit ASM activity (Figure 3H).

## 4. Discussion

One of the key hurdles for the application of drug repurposing is the often weak activity of compounds that limits clinical applications due to unachievable human plasma drug concentration. Of note, three and four drug combinations have successfully been used in the treatment of severe viral infections, including HIV and HCV infections (Abramowicz et al., 2015; Ho, 1995). In addition, drug combination therapy may delay or prevent the development of drug resistance which commonly occur in most infectious diseases (Andersson and Hughes, 2010). To address this low drug potency issue with drug repurposing against EBOV infection, we applied a targeted drug combination approach and identified effective drug combinations that reduced individual drug concentrations by synergistic effect. Inhibitions of two different targets simultaneously by drug combination may cause additional toxicity, compared to the inhibition of one target. However, we did not observe the cytotoxicity in these three drug combinations in this study. This might be due to the lower individual drug concentrations used in these three drug combinations.

To identify the mechanisms of action of the four compounds used in the two sets of 3-drug combinations, we determined the compounds' effects on several pathways known to be required for EBOV entry, including the endocytosis pathway (co-localization with eGFP-

EBOV), cathepsin B/L activities, lysosomal cholesterol accumulation (NPC1 protein function), enlarged lysosome size (damage of lysosome functions), ASM activity, and NAADP stimulated lysosomal calcium release. Toremifene is a selective estrogen receptor modulator approved for treatment of advanced (metastatic) breast cancer (Vogel et al., 2014). It has a long half-life (>24 hrs) in humans. In a repeated-dosing study, the human peak plasma concentration ($C_{max}$) of toremifene ranged from 25 ng/mL to 1,211 ng/mL (0.06 to 2.98 μM) (DeGregorio et al., 2000). It was shown to protect 50% of mice from death caused by EBOV infection. Toremifene's mechanism of action against EBOV was previously suggested to be in a late step in viral entry, excluded from its known effect as an estrogen receptor modulator (Johansen et al., 2013). Although a recent publication reported that toremifene directly binds to EBOV GPs (Zhao et al., 2016), its mechanism of action still remains largely unclear. Our data suggested that toremifene prevents NAADP-stimulated lysosomal calcium release and inhibits ASM activity.

Mefloquine is a synthetic analogue of quinine and approved for treating malaria (Schlagenhauf et al., 2010). Its long half-life in humans (2-4 weeks) makes it a promising candidate of preventive medicine. In human plasma, mefloquine reached a peak concentration of 2,212 ng/mL (5.84 μM) (Karbwang et al., 1994). Mefloquine reportedly inhibits hemozoin formation to kill parasites (Munkhjargal et al., 2012). Like toremifene, we found that it prevents NAADP-stimulated lysosomal calcium release and inhibits ASM function.

Posaconazole belongs to the group of triazole antifungal drugs and is approved for treatment of invasive infections by *Candida*, *Mucor*, and *Aspergillus* species in severely immunocompromised patients (Walsh et al., 2007). Posaconazole has a half-life of 20 hrs in humans. The peak concentration in human plasma is 2,840 ng/ml (4.05 μM) (Kersemaekers et al., 2015). Posaconazole blocks the synthesis of the fungal cell membrane to inhibit growth of the fungi (Munayyer et al., 2004). Our data suggest that posaconazole blocks EBOV infections through multiple mechanisms, including inhibitions of NAADP-stimulated lysosomal calcium release, NPC1 protein function, and ASM activity. Imipramine, an antidepressant drug and NPC1 inhibitor, has been previously reported to be active in inhibition of EBOV entry *in vitro* and showed protection against EBOV infection in a mouse model (Herbert et al., 2015). In our study, 4 μM posaconazole in two sets of three-drug combinations was sufficient to block EBOV infection *in vitro*. The concentrations of all three drugs are achievable in human plasma. Thus, posaconazole used in the three-drug combination presents a promising drug candidate for clinical development to treat EBOV infection.

Clarithromycin is an antibiotic approved for treatment of Gram-positive bacteria and atypical mycobacteria (2008). It has a half-life of 3-7 hrs in humans. The peak human plasma concentration was reported to be 2, 000 ng/m (2.67 μM) (Amini and Ahmadiani, 2005). Its mechanism of action is interfering with protein synthesis in bacteria (Mitui et al., 2013). In our studies, clarithromycin inhibited NAADP-stimulated lysosomal calcium release, which likely explains its anti-EBOV activity.

In summary, we found two sets of three-drug combinations that significantly improved the efficacy of individual drugs against EBOV infection *in vitro* at clinically relevant concentrations previously approved for human use against other indications. The three-drug combinations successfully reduced the required concentrations for each drug based on a synergistic effect. These two 3-drug combinations achieve synergy through functional inhibitions of NPC1 protein, ASM activity, and NAADP-stimulated lysosomal calcium releases. Result of animal and human efficacy studies are still pending, but nonetheless our findings demonstrate that drug repurposing coupled with drug combinations may provide a rapid approach to identify potential therapeutics for the treatment and prevention of EBOV infection.

## Supplementary Material

Refer to Web version on PubMed Central for supplementary material.

## Acknowledgements

## Abbreviations

| | |
|---|---|
| **EBOV** | Ebola virus |
| **NPC1** | Niemann Pick C1 protein |
| **IC$_{50}$** | half-maximum inhibitory concentrations |

## References

Clarithromycin. Tuberculosis (Edinb). 2008; 88:92–95. [PubMed: 18486039]

Abramowicz M, Zuccotti G, Pflomm JM. A 4-Drug Combination (Viekira Pak) for Hepatitis C. Jama-J Am Med Assoc. 2015; 313:1857–1858.

Amini H, Ahmadiani A. Sensitive determination of clarithromycin in human plasma by high-performance liquid chromatography with spectrophotometric detection. J Chromatogr B Analyt Technol Biomed Life Sci. 2005; 817:193–197.

Andersson DI, Hughes D. Antibiotic resistance and its cost: is it possible to reverse resistance? Nat Rev Microbiol. 2010; 8:260–271. [PubMed: 20208551]

Carette JE, Raaben M, Wong AC, Herbert AS, Obernosterer G, Mulherkar N, Kuehne AI, Kranzusch PJ, Griffin AM, Ruthel G, Dal Cin P, Dye JM, Whelan SP, Chandran K, Brummelkamp TR. Ebola virus entry requires the cholesterol transporter Niemann-Pick C1. Nature. 2011; 477:340–U115. [PubMed: 21866103]

Chandran K, Sullivan NJ, Felbor U, Whelan SP, Cunningham JM. Endosomal proteolysis of the Ebola virus glycoprotein is necessary for infection. Science. 2005; 308:1643–1645. [PubMed: 15831716]

Cote M, Misasi J, Ren T, Bruchez A, Lee K, Filone CM, Hensley L, Li Q, Ory D, Chandran K, Cunningham J. Small molecule inhibitors reveal Niemann-Pick C1 is essential for Ebola virus infection. Nature. 2011; 477:344–U122. [PubMed: 21866101]

DeGregorio MW, Wurz GT, Taras TL, Erkkola RU, Halonen KH, Huupponen RK. Pharmacokinetics of (deaminohydroxy)toremifene in humans: a new, selective estrogen-receptor modulator. Eur J Clin Pharmacol. 2000; 56:469–475. [PubMed: 11049009]

Garcia M, Cooper A, Shi W, Bornmann W, Carrion R, Kalman D, Nabel GJ. Productive Replication of Ebola Virus Is Regulated by the c-Abl1 Tyrosine Kinase. Sci Transl Med. 2012:4.

Herbert AS, Davidson C, Kuehne AI, Bakken R, Braigen SZ, Gunn KE, Whelan SP, Brummelkamp TR, Twenhafel NA, Chandran K, Walkley SU, Dye JM. Niemann-Pick C1 Is Essential for Ebolavirus Replication and Pathogenesis In Vivo. Mbio. 2015:6.

Ho DD. Time to hit HIV, early and hard. N Engl J Med. 1995; 333:450–451. [PubMed: 7616996]

Jae LT, Brummelkamp TR. Emerging intracellular receptors for hemorrhagic fever viruses. Trends Microbiol. 2015; 23:392–400. [PubMed: 26004032]

Johansen LM, Brannan JM, Delos SE, Shoemaker CJ, Stossel A, Lear C, Hoffstrom BG, Dewald LE, Schornberg KL, Scully C, Lehar J, Hensley LE, White JM, Olinger GG. FDA-approved selective estrogen receptor modulators inhibit Ebola virus infection. Sci Transl Med. 2013; 5:190ra179.

Karbwang J, Na Bangchang K, Thanavibul A, Back DJ, Bunnag D, Harinasuta T. Pharmacokinetics of mefloquine alone or in combination with artesunate. Bull World Health Organ. 1994; 72:83–87. [PubMed: 8131255]

Kersemaekers WM, van Iersel T, Nassander U, O'Mara E, Waskin H, Caceres M, van Iersel ML. Pharmacokinetics and safety study of posaconazole intravenous solution administered peripherally to healthy subjects. Antimicrob Agents Chemother. 2015; 59:1246–1251. [PubMed: 25512407]

Kouznetsova J, Sun W, Martinez-Romero C, Tawa G, Shinn P, Chen CZ, Schimmer A, Sanderson P, McKew JC, Zheng W, Garcia-Sastre A. Identification of 53 compounds that block Ebola virus-like particle entry via a repurposing screen of approved drugs. Emerg Microbes Infect. 2014; 3:e84. [PubMed: 26038505]

Madrid PB, Chopra S, Manger ID, Gilfillan L, Keepers TR, Shurtleff AC, Green CE, Iyer LV, Dilks HH, Davey RA, Kolokoltsov AA, Carrion R Jr. Patterson JL, Bavari S, Panchal RG, Warren TK, Wells JB, Moos WH, Burke RL, Tanga MJ. A systematic screen of FDA-approved drugs for inhibitors of biological threat agents. PLoS One. 2013; 8:e60579. [PubMed: 23577127]

Miller ME, Adhikary S, Kolokoltsov AA, Davey RA. Ebolavirus requires acid sphingomyelinase activity and plasma membrane sphingomyelin for infection. J Virol. 2012; 86:7473–7483. [PubMed: 22573858]

Mitui M, Khokhar SK, Leos NK, Doern CD, Park JY. Helicobacter pylori 23S rRNA Gene Sequencing for the Identification of Mutations Associated with Clarithromycin Resistance in FFPE Samples. Lab Invest. 2013; 93:373a–373a.

Moller-Tank S, Maury W. Ebola virus entry: a curious and complex series of events. PLoS Pathog. 2015; 11:e1004731. [PubMed: 25928849]

Munayyer HK, Mann PA, Chau AS, Yarosh-Tomaine T, Greene JR, Hare RS, Heimark L, Palermo RE, Loebenberg D, McNicholas PM. Posaconazole is a potent inhibitor of sterol 14 alpha-demethylation in yeasts and molds. Antimicrob Agents Chemother. 2004; 48:3690–3696. [PubMed: 15388421]

Munkhjargal T, AbouLaila M, Terkawi MA, Sivakumar T, Ichikawa M, Davaasuren B, Nyamjargal T, Yokoyama N, Igarashi I. Inhibitory Effects of Pepstatin A and Mefloquine on the Growth of Babesia Parasites. Am J Trop Med Hyg. 2012; 87:681–688. [PubMed: 22890034]

Sakurai Y, Kolokoltsov AA, Chen CC, Tidwell MW, Bauta WE, Klugbauer N, Grimm C, Wahl-Schott C, Biel M, Davey RA. Ebola virus. Two-pore channels control Ebola virus host cell entry and are drug targets for disease treatment. Science. 2015; 347:995–998. [PubMed: 25722412]

Schlagenhauf P, Adamcova M, Regep L, Schaerer MT, Rhein HG. The position of mefloquine as a 21(st) century malaria chemoprophylaxis. Malaria J. 2010:9.

Sun W, Sanderson P, Zheng W. Drug combination therapy increases successful drug repositioning. Drug Discov Today. 2016

Tscherne DM, Manicassamy B, Garcia-Sastre A. An enzymatic virus-like particle assay for sensitive detection of virus entry. J Virol Methods. 2010; 163:336–343. [PubMed: 19879300]

Vogel CL, Johnston MA, Capers C, Braccia D. Toremifene for Breast Cancer: A Review of 20 Years of Data. Clin Breast Cancer. 2014; 14:1–9. [PubMed: 24439786]

Walsh TJ, Raad I, Patterson TF, Chandrasekar P, Donowitz GR, Graybill R, Greene RE, Hachem R, Hadley S, Herbrecht R, Langston A, Louie A, Ribaud P, Segal BH, Stevens DA, van Burik JA, White CS, Corcoran G, Gogate J, Krishna G, Pedicone L, Hardalo C, Perfect JR. Treatment of invasive aspergillosis with posaconazole in patients who are refractory to or intolerant of conventional therapy: an externally controlled trial. Clin Infect Dis. 2007; 44:2–12. [PubMed: 17143808]

Wang Y, Jadhav A, Southal N, Huang R, Nguyen DT. A grid algorithm for high throughput fitting of dose-response curve data. Curr Chem Genomics. 2010; 4:57–66. [PubMed: 21331310]

Xu M, Liu K, Southall N, Marugan JJ, Remaley AT, Zheng W. A high-throughput sphingomyelinase assay using natural substrate. Anal Bioanal Chem. 2012a; 404:407–414. [PubMed: 22710568]

Xu M, Liu K, Swaroop M, Porter FD, Sidhu R, Firnkes S, Ory DS, Marugan JJ, Xiao J, Southall N, Pavan WJ, Davidson C, Walkley SU, Remaley AT, Baxa U, Sun W, McKew JC, Austin CP, Zheng W. delta-Tocopherol reduces lipid accumulation in Niemann-Pick type C1 and Wolman cholesterol storage disorders. J Biol Chem. 2012b; 287:39349–39360. [PubMed: 23035117]

Zhao Y, Ren J, Harlos K, Jones DM, Zeltina A, Bowden TA, Padilla-Parra S, Fry EE, Stuart DI. Toremifene interacts with and destabilizes the Ebola virus glycoprotein. Nature. 2016; 535:169–172. [PubMed: 27362232]

**Highlights**

- Drug combinations may enable clinical application by reducing individual drug concentrations for inhibiting EBOV infection.

- 795 pairs of three-drug combinations of FDA-approved drugs were screened for anti-Ebola virus activity.

- Two sets of clinical useful three-drug combinations were validated for inhibition of live Ebola virus infection.

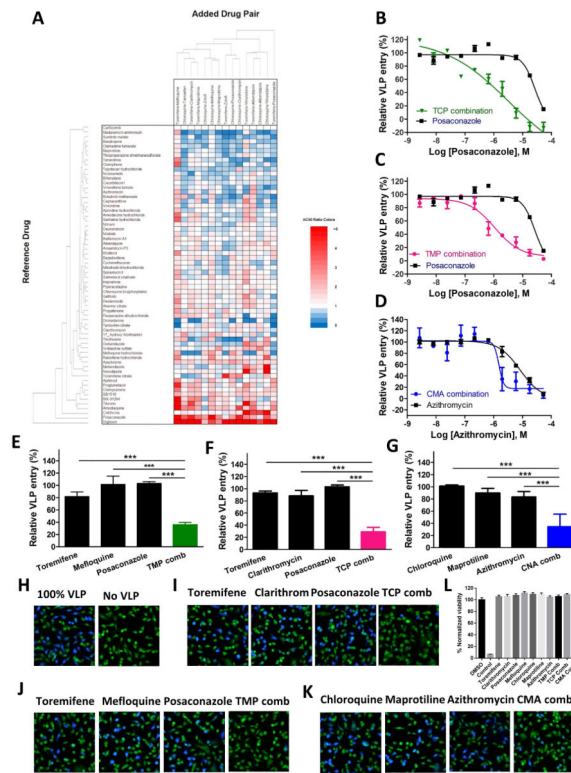- Mechanisms of action of these drugs were identified in affecting host-pathogen interactions.

**Fig. 1. Identifications of three-drug synergistic combinations from screening of FDA-approved drugs in the Ebola entry assay**

(**A**) Heat map of triple drug combinations. Rows enumerate drug 1, columns enumerate drugs 2, 3 and heat map elements are ratios defined as $AC_{50}$ (drug 1 alone)/$AC_{50}$ (drugs 1 + 2 + 3). Color coding: Red = positive synergy (drug triple is more potent than drug 1 alone), white = no synergy (drug triple is equipotent to drug 1 alone), and blue = negative synergy (drug triple is less potent than drug 1 alone). (**B-D**) Shown are dose-response curves with respect to selected drugs. Three-drug combinations (green, red, or blue) verse single drug (black). TCP (0.15 μM toremifene, 2 μM clarithromycin, and 4 μM posaconazole); TMP (0.15 μM toremifene, 2 μM mefloquine, and 4 μM posaconazole); CMA (2 μM chloroquine, 1 μM maprotiline, and 1 μM azithromycin). 0.15 μM toremifene plus 2 μM clarithromycin and 0.15 μM toremifene plus 2 μM mefloquine sensitized the third drug posaconazole from $IC_{50}$ of 24.9 μM (95% CI: 11.6 to 53.5 μM) in the single drug application to 0.97 μM (95% CI: 0.35 to 2.69 μM) and 1.08 μM (95% CI: 0.53 to 2.22 μM) in the three-drug combination, respectively. 2 μM chloroquine with 1 μM maprotiline improved azithromycin from $IC_{50}$ of 8.10 μM (95% CI: 4.82 to 13.6 μM) in the single drug application to 1.53 μM (95% CI: 0.32 to 7.28 μM) in the three-drug combination. (**E-G**) Percentage of Ebola VLP inhibition at dose of each individual drug or three-drug combination. (**H-K**) Represented images of the inhibition of Ebola VLP entry by TCP, TMP and CMA using a high content assay. Magnification is x 20. (**L**) Cytotoxicity of individual drug and three-drug combinations. Cytotoxic control is 100 μM mefloquine. All experiments were performed in triplicate and data are representative of at least two independent experiments. Data are represented as mean±s.e.m. For D, E and F, ***$P$ 0.001. $P$ value indicates that the statistical significance was measured by Student's t-test.
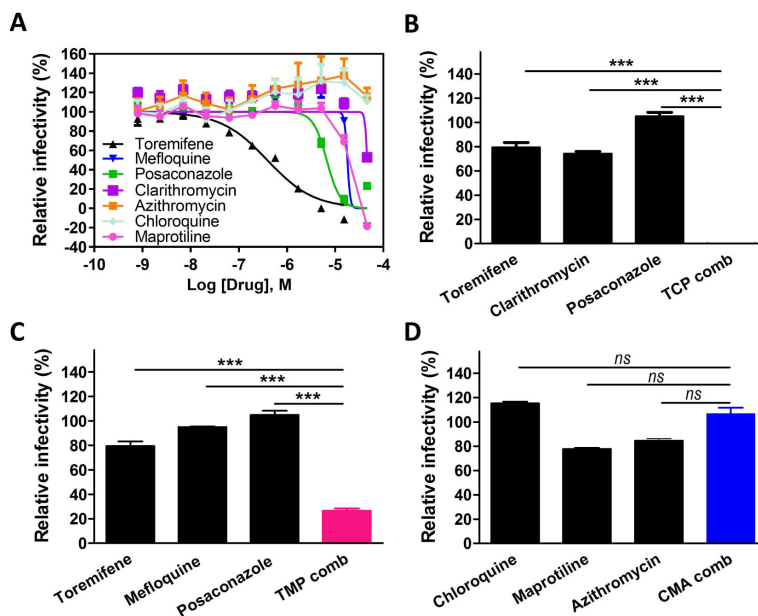
**Fig. 2. Synergistic inhibition of infection of Ebola live virus in Vero E6 cells by three-drug combinations**

**(A)** Confirmatory dose-response curves of toremifene (dark line), mefloquine (blue line), posaconazole (green line), and clarithromycin (purple line) in inhibiting EBOV in Vero E6 cells using eGFP-EBOV assay. **(B-D)** Synergistic inhibition of EBOV infection by three-drug combination: TCP (0.15 μM toremifene, 2 μM clarithromycin and 4 μM posaconazole), TMP (0.15 μM toremifene, 2 μM mefloquine and 4 μM posaconazole), and CMA (2 μM chloroquine, 1 μM maprotiline and 1 μM azithromycin). All experiments were performed in triplicate and data are representative of at least two independent experiments. Data are represented as mean±s.e.m. For B, C and D, ***$P$ 0.001. ns = difference is not statistically significant. $P$ value indicates that the statistical significance was measured by Student's t-test.
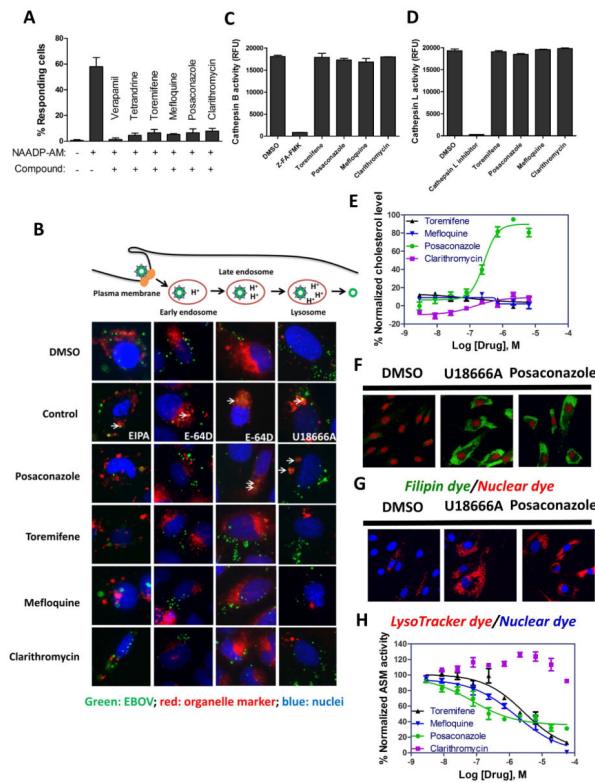
**Fig. 3. Assessment of mechanisms of drugs in perturbing Ebola-host interactions**

**(A)** Inhibition of NAADP-AM stimulated calcium release by toremifene, mefloquine, posaconazole, and clarithromycin. Fibroblasts were loaded with NucBlue and Cal-520 (a calcium dye), treated with indicated drugs and then stimulated with NAADP-AM or HHBS. Cells showing $F_{max}/F_0 > 2$ ($F_{max}$: maximum fluorescence intensity; $F_0$: mean fluorescence intensity before stimulation) were counted as responsive cells. 150 cells were analyzed for each treatment. **(B)** Colocalization images of eGFP-Ebola with RFP-Lck (plasma membrane), RFP-Rab5a (early endosome), RFP-Rab7a (late endosome) or RFP-LAMP1 (lysosome). U2OS cells were treated with DMSO, EIPA, E-64D, U18666A, posaconazole, toremifene, mefloquine or clarithromycin (green: EBOV; red: organelle marker; blue: nuclei). **(C and D)** Drug effects on protease activities of cathepsin B and L. Recombinant cathepsin B or cathepsin L were treated with DMSO, Z-FA-FMK, cathepsin L inhibitor, toremifene, mefloquine, posaconazole, or clarithromycin. **(E)** Dose-response curves of toremifene (dark line), mefloquine (blue line), posaconazole (green line), and clarithromycin (purple line) in Amplex-red cholesterol assay in Hela cells. **(F)** Cholesterol accumulation induced by U18666A and posaconazole in fibroblasts (green: filipin; red: nuclei). **(G)** Lysosome enlargement induced by U18666A and posaconazole in fibroblasts (red: lysotracker; blue: nuclei). **(H)** Dose-response curves of toremifene (dark line), mefloquine (blue line), posaconazole (green line), and clarithromycin (purple line) in acid sphingomyelinase (ASM) assay in Hela cells. All experiments were performed in triplicate and data are representative of at least two independent experiments. Data are represented as mean±s.e.m.

**Table 1**

Efficacy and human plasma concentrations of seven drugs that synergistically blocked Ebola VLP entry

| Drug name | IC$_{50}$ (μM) | IC$_{90}$ (μM) | C$_{comb}$ (μM) | C$_{max}$ $^a$ (μM) | C$_{mean}$ $^b$ (μM) | Approved indication | Mechanism of action (MOA) for approved indication |
|---|---|---|---|---|---|---|---|
| Toremifene | 0.57 | 3.73 | 0.15 | 2.98 | 2.35 | Anticancer | Estrogen receptor modulator |
| Chloroquine | 15.3 | 133 | 2 | 2.02 | 0.2-1.2 | Antimalarial | Hemozoin formation inhibitor |
| Maprotiline | 2.55 | 12.1 | 1 | 0.94 | 0.4-1.4 | Antidepressant | Adrenergic uptake inhibitors and histamine antagonist |
| Mefloquine | 6.45 | 14.2 | 2 | 5.84 | 2.6 | Antimalarial | Hemozoin formation inhibitor |
| Azithromycin | 2.79 | 15.8 | 1 | 1.34 | 0.05-1.3 | Antimicrobial | Protein synthesis inhibitor |
| Clarithromycin | 4.33 | 15.1 | 2 | 2.67 | 2.7 | Antimicrobial | Protein synthesis inhibitor |
| Posaconazole | 24.9 | 53.1 | 4 | 4.05 | 2.3-3.1 | Antifungal | Membrane-bound enzyme inhibitor |

Note: IC$_{50}$ and IC$_{90}$, mean half-maximum inhibitory concentrations and 90% inhibitory concentrations determined from at least 3 independent experiments in Ebola VLP assays.

$^a$C$_{max}$, were derived from literature, see discussion.

$^b$C$_{mean}$, were derived from literature, see discussion.

**Table 2**

Comparison of anti-EBOV activity of drugs in Ebola VLP entry and EBOV infection assays

| Drug Name | Ebola VLP | | | Ebola live virus | | |
|---|---|---|---|---|---|---|
| | $IC_{50}$ (µM) | 95% CI (µM) | Max Inh. (%) | $IC_{50}$ (µM) | 95% CI (µM) | Max Inh. (%) |
| Toremifene | 0.57 | 0.36-0.73 | 98 | 0.53 | 0.35-0.80 | 98 |
| Posaconazole | 24.9 | 11.6-53.5 | 77 | 6.31 | 5.24-8.48 | 92 |
| Mefloquine | 6.45 | 5.39-7.71 | 94 | 16.6 | - | 100 |
| Clarithromycin | 4.33 | 3.75-5.00 | 100 | 42 | - | 47 |
| Chloroquine | 15.3 | 10.9-30.6 | 98 | ND | ND | 0 |
| Maprotiline | 2.55 | 2.13-3.05 | 100 | 15 | - | 100 |
| Azithromycin | 2.79 | 2.30-3.44 | 100 | ND | ND | 0 |

Note: 95% CI, 95% confidence interval. Max. Inh., maximal inhibition. -, compounds with wide 95% CI. ND, compounds were not active at up to 53 µM. n=3.